Supporting Information

Huillard et al. 10.1073/pnas.1117255109

SI Materials and Methods

Transgenic Mice. *BRaf*^{CA} (1) and *Ink4a-Arf*$^{-/-}$ (National Cancer Institute, NCI repository) or *Ink4a-arf*$^{LoxP/LoxP}$ (2) mouse lines were intercrossed to generate *BRaf*$^{CA/+}$*Ink4a-Arf*$^{-/-}$ or *BRaf*$^{CA/+}$ *Ink4a-Arf*$^{LoxP/LoxP}$ animals. *BRaf*$^{CA/+}$*; Ink4a-Arf*$^{-/-}$ mice were crossed to hGFAP-cre mice (Jackson Laboratories) to generate *hGFAP-cre;BRaf*$^{CA/+;}$ *Ink4a-Arf*$^{-/-}$ mice or to *Ink4a-Arf*$^{-/-}$ to generate *BRaf*$^{CA/+}$*; Ink4a-Arf*$^{-/-}$ mice. All animal studies (mouse procedures and husbandry) were performed according to University of California San Francisco guidelines under the institutional animal care and use committee.

Proliferation and Differentiation Assays for Murine Neural Progenitors. For proliferation and apoptosis assays, neurosphere cultures were dissociated and plated at a density of 10^4 cells per well onto eight-well polylysine/laminin-coated slides (BD). Cells were allowed to adhere for 24 h and fixed with 4% (wt/vol) paraformaldehyde (PFA). Bromodeoxyduridine (BrdU, 10 μM) was added 30 min before fixation. For differentiation assays, cells on coated slides were switched to growth factor-free medium 24 h after plating. Cultures were maintained for 7 d and fixed in 4% PFA. Cells were immunostained using standard protocols with anti-BrdU (1/100; BD Pharmingen), anticleaved caspase 3 (1/500; Cell Signaling), anti-GFAP (1/2,000; Sigma), anti–βIII-tubulin (TuJ1, 1/1,000; Covance), anti-O4 (1/100; Chemicon), and anti-Ki67 (1/500; BD Pharmingen).

Modification of Tumor Cells with Firefly Luciferase-Expressing Reporter. DBTRG05-MG, 10776, and AM-38 cells were transduced with a lentivirus encoding the firefly luciferase (Fluc) under the control of the spleen focus forming virus (SFFV) promoter, as previously described (3). Cells were screened for transfection efficiency by treatment with luciferin (D-luciferin potassium salt, 150 mg/kg; Gold Biotechnology) in vitro and examination by a IVIS Lumina system (Xenogen). More than 80% of cells were transfected.

Flow Cytometry. To examine G1 cell cycle arrest induction by PD0332991, 1.0×10^6 cells were plated into 6-cm dishes and allowed to adhere overnight. Cells were treated with PD0332991 (1 μM in 50 mM sodium lactate, pH 4) for 18 h. Equal volumes of sodium lactate were used as treatment controls. Cells were pulsed with 10 μmol/L bromodeoxyuridine (BrdU) for 1 h, trypsinized, and centrifuged. Cells were fixed and stained using the FITC BrdU Flow kit (Pharmingen), counterstained with 7-amino-actinomycin D (7-AAD), and analyzed by flow cytometry in a BD FACSCalibur instrument using FlowJo 8.8 software.

Western Blotting. Total cell lysate was collected from asynchronously proliferating cells in buffer (Cell Signaling) supplemented with proteinase (Roche) and phosphatase (Sigma) inhibitor mixtures, resolved by SDS/PAGE, and then immunoblotted using standard techniques. Primary antibodies for Rb (sc-7905), Phospho-Rb-Ser780 (sc-12901), and ERK were obtained from Santa Cruz Biotechnology. Antibodies specific for RB (4H1), phospho-RB (Ser780), AKT, phospho-AKT (Ser473), MEK1/2, phospho-MEK1/2, phospho-ERK, CDK4, and CDK6 were obtained from Cell Signaling Technologies. P16 antibody was from BD Pharmingen, β-tubulin antibody was from Upstate Biotechnologies.

In Vivo Bioluminescence Imaging (BLI). In vivo BLI was performed with the IVIS Lumina system (Xenogen) coupled to the LivingImage data-acquisition software (Xenogen). Mice were anesthetized with 100 mg/kg of ketamine and 10 mg/kg of xylazine and imaged 10 min after i.p. injection of luciferin (D-luciferin potassium salt, 150 mg/kg; Gold Biotechnology). Signal intensity was quantified within a region of interest over the mouse head, as defined by the LivingImage software. Bioluminescence measurements for each animal were normalized against corresponding readings obtained at the beginning of therapy.

Histological Analyses. Brains were perfused with 4% paraformaldehyde (PFA) and postfixed overnight. Brains were either cryoprotected in sucrose 15% and embedded in OCT (TissueTek, Sakura) or embedded in paraffin. Sections (14-μm cryosections or 5-μm paraffin sections) were used for immunohistochemical and H&E stainings. For immunohistochemical stainings, frozen or paraffin sections were stained using the EnVision kit (Dako) following the manufacturer's instructions. The primary antibodies used were: anti-Olig2 (1/1,000; Chemicon), antiphospho-ERK (1/500; Cell Signaling), anti-GFAP (1/2,000; Dako), anti-Ki67 (2 μg/mL; Ventana; 790-7264), and anti-Nestin (1/1,000; BD Pharmingen). Sections were counterstained with Mayer's hematoxylin (Sigma).

Statistical Analyses. GraphPad Prism software was used to generate tumor growth curves from bioluminescence image and differences between growth curves were calculated by unpaired *t* test. The Kaplan–Meier estimator and GraphPad Prism software were used to generate survival curves. Differences between survival curves were calculated using a log-rank test. Unpaired *t* test was used to determine differences between numbers of marker-positive cells in Figs. 2, 4, and 5.

1. Dankort D, et al. (2007) A new mouse model to explore the initiation, progression, and therapy of BRAFV600E-induced lung tumors. *Genes Dev* 21:379–384.
2. Aguirre AJ, et al. (2003) Activated Kras and Ink4a/Arf deficiency cooperate to produce metastatic pancreatic ductal adenocarcinoma. *Genes Dev* 17:3112–3126.
3. Sarkaria JN, et al. (2007) Identification of molecular characteristics correlated with glioblastoma sensitivity to EGFR kinase inhibition through use of an intracranial xenograft test panel. *Mol Cancer Ther* 6:1167–1174.

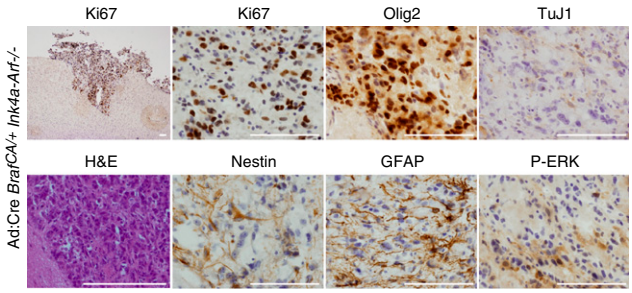

Fig. S1. Histological and immunohistochemical characteristics of Ad-*cre* $BRaf^{CA/+}$ *Ink4a-Arf*$^{-/-}$ tumors. (Scale bars, 100 μm.)

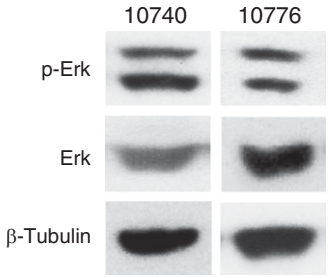

Fig. S2. Western blot analysis of the expression of ERK and phospho-ERK (p-ERK) in GFAP-cre $BRaf^{CA/+}$ *Ink4a-Arf*$^{-/-}$ tumors (line 10740) Ad-*cre* $BRaf^{CA/+}$ *Ink4a-Arf*$^{-/-}$ (line 10776).

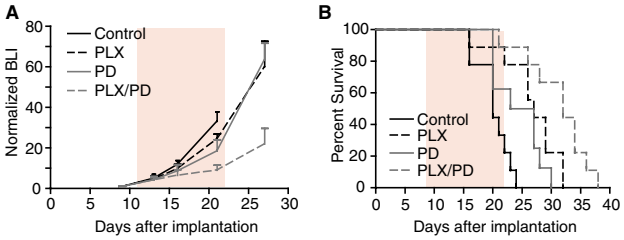

Fig. S3. Therapeutic response of orthotopic AM-38 human astrocytoma xenografts to BRAF and CDK4/6 inhibitors. Intracranial tumors generated from the AM-38 astrocytoma line were treated with PD0332991, PLX4720, or PLX4720 + PD0332991 therapies for 14 consecutive days (pink area). (*A*) Bioluminescence imaging (BLI). *P* values for differences between growth curves on day 21 were calculated. $P = 0.0121$ for control vs. PLX + PD combination therapy. There are no statistically significant differences in tumor growth rate between control vs. PLX ($P = 0.5027$) or PD ($P = 0.1746$). Although there is a trend for the combination being superior, there are no significant differences in tumor growth rate between PD or PLX vs. PD/PLX treatment groups: $P = 0.0506$ for combination vs. PLX, and $P = 0.1820$ for combination vs. PD. (*B*) Kaplan–Meier survival curves; $P = 0.0028$ for control vs. PLX, $P = 0.0005$ for control vs. PD0332991; $P < 0.001$ for PLX or PD vs. PLX4720 + PD0332991 combination therapy.

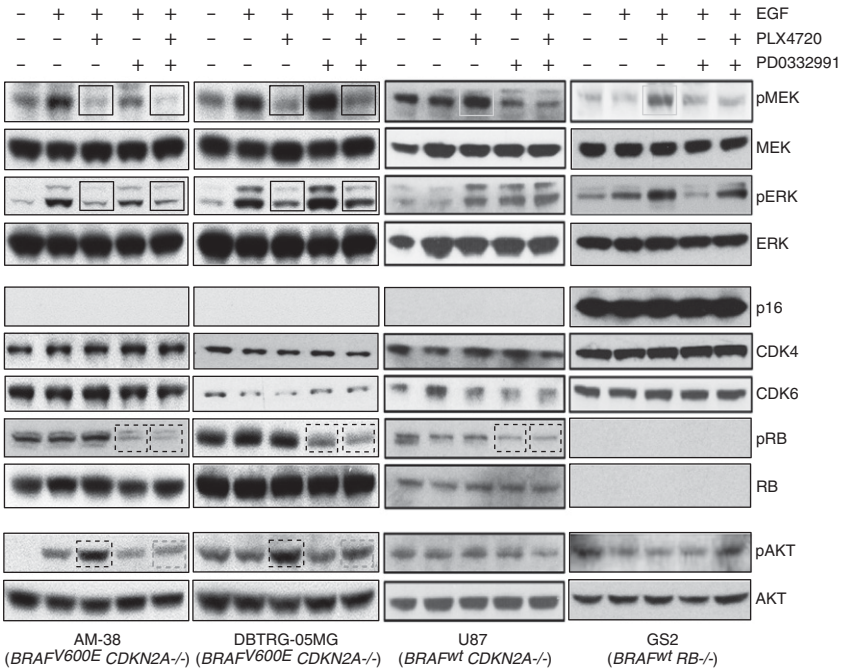

Fig. S4. Characterization of the activated signaling pathways following $BRAF^{V600E}$ and CDK4/6 inhibition in AM-38, DBTRG05-MG, U87, and GS2 cell lines. Cells were serum starved for 16 h and treated for 1 h with either EGF (25 ng/mL), EGF (25 ng/mL) + PLX4720 (10 mM), EGF (25 ng/mL) + PD0332991 (10 mM), or EGF + PLX4720 (10 mM) + PD0332991 (10 mM). Solid black rectangles indicate the expected pMAPK and pERK suppressive effects following BRAF inhibition with PLX4720. Note that pMEK and pERK are unexpectedly induced by PLX4720 in U87 and GS2 lines (solid gray rectangles). Dotted black rectangles indicate the expected pRB suppressive effect of PD0332991 in the *p16*-deficient AM-38, DBTRG05-MG, and U87 cells. We noted an unexpected induction of pAKT following PLX4720 treatment on $BRAF^{V600E}$ AM-38 and DBTRG05-MG cells (dashed black rectangles), and this induction was suppressed by cotreatment with PD0332991 (dashed gray rectangles).

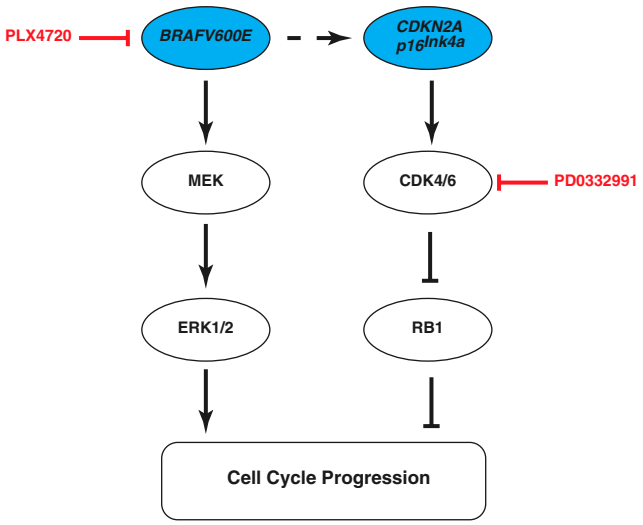

Fig. S5. $BRAF^{V600E}$ and p16 pathway interactions and therapeutic implications. Diagram depicts relevant mutations in a subset of pediatric astrocytoma (blue ovals). Present findings suggest that in neural progenitors, heterozygous $BRAF^{V600E}$ mutation alone leads to induction of p16 expression (dashed arrow), which in turn results in enhanced RB1 activity and inhibition of cell cycle progression. We speculate this provides selective pressure for biallelic inactivation of *CDKN2A* in human astrocytomas. Inhibitors PLX4720 and PD0332991 show individual and additive therapeutic effects in genetically faithful preclinical models.